CHIN. PHYS. LETT. Vol. 37, No. 1 (2020) 010301 **Express Letter**

Critical Scaling Behaviors of Entanglement Spectra *

Qi-Cheng Tang(唐启承)[1,2], Wei Zhu(朱伟)[1,2]**

[1]*School of Science, Westlake University, Hangzhou 310024*

[2]*Institute of Natural Sciences, Westlake Institute of Advanced Study, Hangzhou 310024*

(Received 25 October 2019)

We investigate the evolution of entanglement spectra under a global quantum quench from a short-range correlated state to the quantum critical point. Motivated by the conformal mapping, we find that the dynamical entanglement spectra demonstrate distinct finite-size scaling behaviors from the static case. As a prototypical example, we compute real-time dynamics of the entanglement spectra of a one-dimensional transverse-field Ising chain. Numerical simulation confirms that the entanglement spectra scale with the subsystem size l as $\sim l^{-1}$ for the dynamical equilibrium state, much faster than $\propto \ln^{-1} l$ for the critical ground state. In particular, as a byproduct, the entanglement spectra at the long time limit faithfully gives universal tower structure of underlying Ising criticality, which shows the emergence of operator-state correspondence in the quantum dynamics.

PACS: 03.65.Ud, 11.25.Hf DOI: 10.1088/0256-307X/37/1/010301

Conformal field theory (CFT)[1] has become a profitable tool as a diagnosis of critical phenomena in two-dimensional statistical models. In the equilibrium case, the conformal invariance at the critical point sets rigid constrains on physical properties by a set of conformal data including the central charge, conformal dimensions and operator product expansion coefficients. In the past decades, great success has been achieved in condensed matter physics, especially for minimal models with a finite number of primary scaling operators (irreducible representations of the Virasoro algebra).[2–6]

In general, due to gaplessness nature, massive entanglement should play a vital role at or around the critical point. One remarkable achievement is[7–34] that CFT provides a novel way to connect the quantum entanglement and critical phenomena. It is found that the conformal invariance in critical ground states results in a universal scaling of the entanglement entropy depending on the central charge c.[8–10,13,16] Interestingly, by extending this idea, the entropy can be applied to identify quantum critical points in higher dimensions.[13,16,35–37] Besides the entropy, other entanglement-based measures also attract a great deal of attention. The eigenvalues of reduced density matrix, called entanglement spectrum (ES), is such an example, which contains much richer information than the entropy.[38,39] In addition to the evidences in topological gapped systems,[40–43] the ES is also proposed to describe the quantum critical point.[15,44–51] However, compared to the well-established boundary law for gapped states, much less is known about the critical behavior of the ES,[52,53] which casts doubt on direct application of the ES in the critical systems.

Beyond equilibrium, quantum dynamics attracts considerable attention recently, particular in approaching to steadiness and thermalization. Universal entanglement structures are expected to leave some marks in the dynamic process, e.g., central charge c controls the growth of entropy.[11,17] However, novel example[8] is still rare, and to extract the conformal data in microscopic models is a challenging task.[14,25,27,32]

In this Letter, we present a systematical study of dynamics of the ES in the process of quantum quench. Inspired by the CFT, we compute the real-time dynamics of the 1D transverse-field Ising (TFI) model, through a protocol by quenching from a gapped state to the critical point. We successfully establish that quantum quench dynamics indeed encodes universal signatures of quantum critical point. Firstly, the ES at long time dynamics converges to the CFT operators as $\propto l^{-1}$, which is much faster than that for critical ground state as $\propto \ln^{-1} l$. Secondly, fast convergence allows us to extract conformal information including conformal dimensions and related degeneracy, which unambiguously pin down the underlying nature of quantum critical point ($c = 1/2$ Ising theory in our case). These key findings open a door to extract quantum criticality in many-body dynamics.

Entanglement spectrum in two dimensional conformal field theory. We consider the global quantum quench to a critical point that is governed by a CFT ($H(t > 0) = H_{\rm CFT}$), and the initial state $|\psi_0\rangle$ is chosen to be the ground state of a gapped Hamiltonian $H(t = 0) = H_0$. In this work, we study the geometry of a semi-infinite chain. In boundary CFT,[27,28,30] the corresponding time-dependent density matrix $\rho(t) = e^{-iHt}|\psi_0\rangle\langle\psi_0|e^{+iHt}$ can be repre-

*Supported by the start-up funding from Westlake University, and the National Natural Science Foundation of China under Grant No 11974288.

**Corresponding author. Email: zhuwei@westlake.edu.cn

sented geometrically by a semi-infinite strip in complex plane with width $\tau = \Im(z) \in [-\frac{\beta}{4}, \frac{\beta}{4}]$ and length $x = \Re(z) \in [0, +\infty)$. The entanglement dynamics of a finite subsystem $A \equiv [0, l]$ is our focus. The reduced density matrix $\rho_A(t)$ can be calculated by sewing together the points which are not in A (the geometric distribution of partial trace). This can be achieved by conformally mapping the semi-infinite strip in z-plane onto the annulus in w-plane, with $w = f(z)$, as shown in Fig. 1. On the annulus, the entanglement Hamiltonian $H_{\rm E} = -\ln \rho_A$ can be considered as the generator of translation along the $v = \Im w$ direction, i.e. $H_{\rm E}$ has the same structure with the CFT Hamiltonian $H_{\rm CFT}$. Then $H_{\rm E}$ in original z-plane can be calculated by mapping the CFT Hamiltonian back to the z-plane.[28,30] In this context, one can obtain the entanglement Hamiltonian for a finite interval A of $[0, l]$ in a semi-infinite critical ground state as (in the static case)

$$H_{\rm E}(t=0) = \int_A \frac{\pi(l^2 - x^2)}{l} H_{\rm CFT}(x) dx. \tag{1}$$

While in the dynamic case, we figure out the entanglement Hamiltonian in the long time limit in the process of quantum quench as[28,30] (for details see the Supplemental Material)

$$H_{\rm E}(t \to \infty) \simeq \beta \int_A H_{\rm CFT}(x) dx. \tag{2}$$

Here we stress that, although $H_{\rm E}$ depends on the CFT Hamiltonian density $H_{\rm CFT}(x)$ in both static and dynamic cases, the entanglement Hamiltonian has an additional spatial-dependent envelope function $l^2 - x^2$ in the static case (Eq. (1)), which is in sharp contrast to that in the dynamic case (Eq. (2)). This difference will lead to the influence on the static ES, as we will discuss in the following.

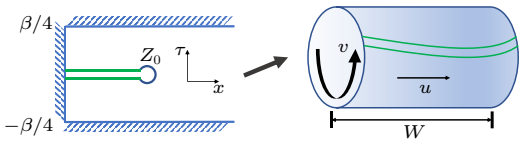

Fig. 1. Conformal mapping from the semi-infinite strip in z-plane to the annulus in w-plane. Left: The global quench of a semi-infinite short-range correlated chain (with correlation length β) is considered as a boundary CFT with $\tau \in [-\frac{\beta}{4}, \frac{\beta}{4}]$. The green lines represent the branch cut $C = \left\{z = x + i\tau; x \in [0, L], \tau \in [-\frac{\beta}{4}, \frac{\beta}{4}]\right\}$. Right: The annulus after conformal mapping $w = f(z)$, where the branch cut C is mapped to a $f(C)$ which connects the two edges of the annulus (see the Supplementary Material for details). The circumference along $v = \Im w$ direction is 2π, and the width of the annulus along the $u = \Re w$ direction is denoted by W.

Another notable difference is that the ES has distinct dependence on the subsystem size l. In CFT, the width of the annulus W along the $u = \Re w$ direction plays an important role in the scaling behavior of ES, through

$$E_i - E_j = \frac{2\pi^2(\Delta_i - \Delta_j)}{W}, \tag{3}$$

where E_i is the ES that is the eigenvalues of $H_{\rm E}$, and Δ_i is conformal dimension of the CFT. The width W can be obtained by a straightforward calculation $W = \Re\mathcal{W} = \frac{1}{2}(\mathcal{W} + \overline{\mathcal{W}})$ with $\mathcal{W} = f(i\tau + L - \epsilon) - f(i\tau)$. For critical ground states on a semi-infinite chain, one obtains the following dependence in the static case

$$W(t=0) = 2\ln\frac{l}{\epsilon}, \tag{4}$$

where ϵ is a scale relevant cut-off. This makes the entropy at the critical point $S \propto \ln l$, and the ES proportional to $E_i - E_j \propto \ln^{-1} l$. In particular, in the case of global quenching a semi-infinite chain considered in the present work, the width W shows the following behaviors (also see the Supplementary Material):[28,30]

$$W(t>0) \sim \begin{cases} \frac{2\pi}{\beta} t, & t < l, \\ \frac{2\pi}{\beta} l, & t \to \infty. \end{cases} \tag{5}$$

Hence, the ES of dynamical equilibrium state approximates to the CFT scaling spectrum with speed $\propto l^{-1}$. Moreover, one can obtain that W approaches steadiness exponentially after the saturated time $t = l$ as (also see the Supplementary Material)

$$W(t > l) \simeq W(t \to \infty) - \frac{1}{2}\exp[-\frac{4\pi(t-l)}{\beta}], \tag{6}$$

and it is also reflected in the dynamics of EE and ES.

Numerical Results. We test the CFT prediction of entanglement dynamics in the TFI chain under the open boundary condition,

$$H_{\rm TFI} = -\sum_i \sigma_i^x \sigma_{i+1}^x - g\sum_i \sigma_i^z, \tag{7}$$

where σ_i^x, σ_i^z are the Pauli matrices at ith site, and g is the strength of the magnetic field. There exists a quantum phase transition between the ferromagnetic ($g < 1$) and paramagnetic ($g > 1$) phases, and the ground state is gapless only at the critical point $g = 1$. The critical ground state of the TFI chain is described by the minimal model with central charge $c = \frac{1}{2}$, and the corresponding scaling operators are listed in Table 1. The TFI chain can be solved exactly by introducing Jordan–Wigner transformation,[54] and its ES can be calculated from the *correlation matrix*.[55] We consider the ES dynamics during global quench from a ground state of gapped phase of the TFI chain ($g \neq 1$) to the Ising CFT ($g = 1$). The time-dependent ES can be calculated by the time-dependent correlation matrix.[56] In this calculation, the total system size is up to $L = 1024$, and we choose subsystem size $l \ll L$. In the condition of $l \ll L$, when we consider the time domain $t < L$ we can safely neglect the boundary effect from $x \sim L$ on the subsystem $A = [0, l]$.

In addition, we also solve the TFI model using the matrix product state approach, i.e. the time-evolving block decimation (TEBD) technology.[57] The bond dimension is adopted by 1024, and the truncation error is set to be 10^{-8}. For dynamics, the time evolution operator is approximated by using second order Trotter–Suzuki decomposition, and the time step is chosen to be $dt = 0.01$. Under the current convergence criterion, the total system sizes in TEBD calculations are limited to $L \leq 72$.

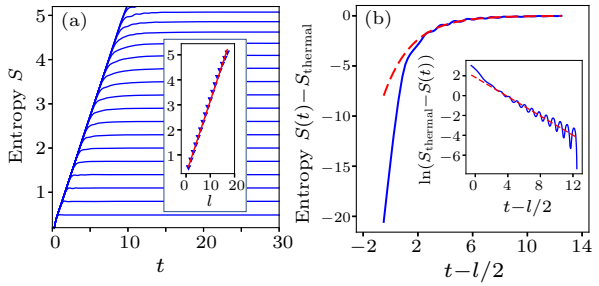

Fig. 2. Entanglement entropy evolution during global quench from gapped phase ($g = 4$) to critical point ($g = 1$) with total system size $L = 512$. Left: Entropy $S(t)$ grows linearly with the "entanglement velocity" $v_{\rm E} \approx 0.52$. Inset: The finite-size saturation leads to a volume law entropy in dynamic equilibrium state. A linear fit (red line) of $S(l) = al + b$ for the numerical data (blue triangle) gives $a = 0.29$ and $b = 0.24$. Right: Entropy $S(t) - S_{\rm thermal}$ for $l = 15 \ll L = 512$ exhibits exponential dependence on $t - l/2$ after reaching the typical time $t \sim l/2$. Inset: A linear fit (red dashed lines) of $\ln[S_{\rm thermal} - S(t)] = a'(t - l/2) + b'$ for the numerical data (blue lines) gives $a' = -0.4844 \pm 0.0078$ and $b' = 1.833 \pm 0.060$.

In Fig. 2, we present the numerical result of the EE evolution during global quench in the TFI chain with total system size $L = 512$. As shown in the left panel, the EE grows linearly with the "entanglement velocity" at early times, then saturated by finite subsystem size l at time $t = l/2$. The inset provides numerical evidence of the resulting volume law by a linear fitting of EE with l. The right panel of Fig. 2 shows an exponential approaching to equilibrium at late times, consistent with Eq. (6).

Now we turn to consider the ES, and we will address how the ES represents the scaling operators in CFT. In CFT, the scaling operators (representations of the corresponding Virasoro algebra) can be obtained by *q-expansion* of the partition function. For the Ising model under the open (free) boundary condition, one can find that there are only two primary scaling operators: the identity I with conformal dimension $\Delta = 0$ and the energy density ϵ with $\Delta = \frac{1}{2}$.[5,6] Their characters can be expanded as follows:

$$\begin{aligned}\chi_I =& q^{-1/48}(1 + q^2 + q^3 + 2q^4 + 2q^5 \\ &+ 3q^6 + 3q^7 + 5q^8 + \cdots) \\ \chi_\epsilon =& q^{1/2-1/48}(1 + q + q^2 + q^3 + 2q^4 + 2q^5 \\ &+ 3q^6 + 3q^7 + 5q^8 + \cdots),\end{aligned} \tag{8}$$

which gives the spectrum of the primary operators and corresponding descendants, each expansion term mq^n represents m-fold degenerate scaling operators with conformal dimension $\Delta_i = n$. The *operator-state correspondence* suggests that the eigenspectrum of (entanglement) Hamiltonian shares the structure of scaling operators, and this relation has been well studied in the energy spectrum of spin chains.[58–61]

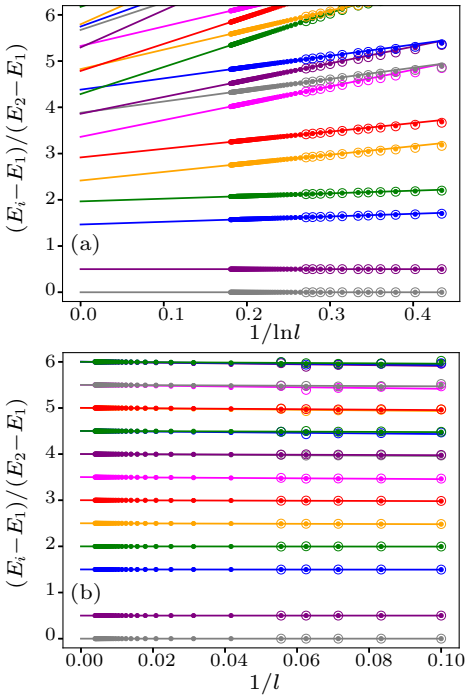

Fig. 3. Entanglement spectra of the TFI model as a function of the subsystem size l. Here we set the total system size $L = 4l$. The solid dots and open circles label the exact solutions and TEBD results, respectively. Upper: Entanglement spectra for the critical ground state ($g = 1$), and the related fitting lines in the form of $a \ln^{-1} l + b$. Lower: Entanglement spectra for global quench from the gapped phase ($g = 4$) to the critical point ($g = 1$). The best fitting lines are in form of $al^{-1} + b$.

The numerical results of the ES of TFI chain for the critical ground state and dynamical equilibrium state are respectively plotted in Fig. 3, which includes the main result of the current work. Here we consider the entanglement cut always located at $l = L/4$ with changing the total system size L. In order to make a direct comparison to the Ising scaling spectrum, we renormalize ES by setting the lowest level to 0 and the second level to 1/2, and show the quantities $(E_i - E_1)/(E_2 - E_1)$ in Fig. 3. Several salient features are found in the ES. Firstly, we identify distinct scaling behaviors of the ES depending on subsystem size l, by comparison of the static ground state and dynamic equilibrium state. As shown in Fig. 3, it is evident that the static ES for critical ground state converges as $\sim \ln^{-1} l$, while for the quantum quench case the ES at late times demonstrates a typical $\sim l^{-1}$ dependence. Physically, this difference can be understood from the CFT results shown in Eqs. (3), (4) and (5). It is worth

noting, this indicates that the ES in quantum quench process converges much faster than that of the critical ground state (for example, in dynamics $l = 10$ (the smallest size we consider) gives $1/l = 0.1$, while in static case $l = 256$ (the largest size we consider) gives $1/\ln l = 0.18$). Such a slow convergence of the ES for the critical ground state is difficult to give reliable conformal information (see below). By comparison, the ES in the quantum quench dynamics easily reaches convergence for extracting the conformal tower structures.

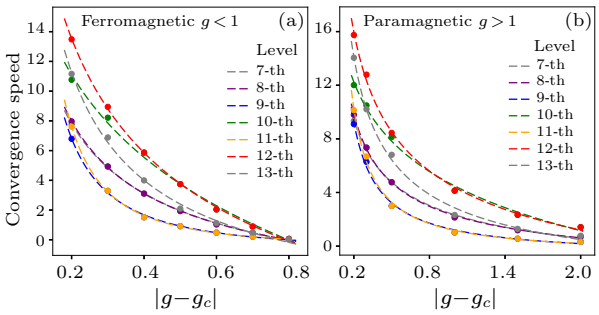

Fig. 4. Dependence of convergence speed to CFT scaling operators on the initial g: for ferromagnetic (left panel) and paramagnetic (right panel) cases. Dots represent the result of convergence speed extracted from the finite-size scaling, and the dashed lines are the result of fitting $v_{\text{converge}} = a|g - g_c|^{\alpha} + b$. Here 7th to 13th levels are plotted.

Table 1. A comparison of the operator content in the Ising CFT ($c = 1/2$) and the scaling of the ES for the static (critical ground state) and dynamic (quantum quench) cases. Here Δ and D are conformal dimension and degeneracy, respectively.

ith level	Sector	CFT		Dynamic ES		Static ES	
		Δ	D	Δ	D	Δ	D
3	ϵ	3/2	1	1.500	1	1.430	1
4	I	2	1	2.000	1	1.930	1
5	ϵ	5/2	1	2.501	1	2.300	1
6	I	3	1	3.001	1	2.800	1
7	ϵ	7/2	1	3.503	1	3.135	1
8	I	4	2	4.001(3)	2	3.635	1
9	ϵ	9/2	2	4.501(5)	2	3.729	1

Secondly, the ES in dynamic process perfectly converges to the CFT expectation, however, the ES of the critical ground state does not. In Table 1, we list the operator content in Ising CFT and the numerical results. In particular, within the numerical uncertainty, the ES of dynamic equilibrium state matches the tower structure of the CFT, for both the conformal dimension Δ_i and its degeneracy. As a comparison, under the proper scaling, the ES of the critical ground state is fail to give conformal information. This can be attributed to the following reasons: (1) The scaling of the ES converges very slowly as $\ln^{-1} l$, which hinders a clear scaled results in the limit of $l \to \infty$. (2) The ES of static critical ground state is strongly influenced by the envelop function in entanglement Hamiltonian (see Eq. (1)).

Thirdly, we stress that the scaling form of the ES is robust, independent of the details of quench dynamics (see the Supplementary Material). Interestingly, it is found that the convergence speed (slope of the finite-size scaling function of ES) indeed relies on the initial conditions. Here we define the convergence speed $v_{\text{converge}} = \frac{E_i - E_j}{\Delta_i - \Delta_j}/F(l)$, where $F(l)$ is the scaling function. In the case of global quench, we have $F(l) = l^{-1}$ and $E_i - E_j = \frac{2\pi^2(\Delta_i - \Delta_j)}{W} = \frac{\beta\pi(\Delta_i - \Delta_j)}{l}$, which gives $v_{\text{converge}} = \beta\pi$. To check the above argument, v_{converge} is extracted and plotted in Fig. 4 with the fitting in form of $\sim|g - g_c|^{\alpha}$. The results of quenching from ferromagnetic ($g < 1$) and paramagnetic ($g > 1$) phases show very similar behaviors, and partially support that v_{converge} is determined by effective temperature. Especially, the differences between different levels become negligible when approaching infinite temperature limit.

Summary and discussion. We have investigated the evolution of entanglement spectra during a global quench. As suggested by boundary conformal field theory, we conclusively show that the entanglement spectra approaches the thermodynamic limit following $\propto l^{-1}$, where l is typical subsystem size. As a comparison, the convergence of entanglement spectra of critical ground state follows $\propto \ln^{-1} l$, much slower than that of the dynamic case. In particular, the entanglement spectra of dynamic equilibrium state encodes the conformal dimensions, which ambiguously pins down the nature of quantum criticality.

These results indicate that, at least in principle, one could obtain critical entanglement content in quantum dynamics, based on finite-size calculations. As an example, we apply the TEBD method on the TFI model, and compare the results with exact solutions in Fig. 3. This additional test implies that, if the correct scaling form is properly applied, numerical solvers on the limited system sizes are potentially able to resolve CFT information. In addition, as we discussed in Fig. 4 and in the Supplementary Material, a fast convergence is possible under optimized quenching parameters. In this context, the out-of-equilibrium scaling form paves a promising road for future study using various numerical methods (e.g. time-dependent density-matrix renormalization group).

This work opens a number of open questions that are deserved to study in future. For example, it would be important to promote our findings to more systems, such as other CFT minimal models and non-integrable models, and related work is still in progress. How the scaling behaviors change under the influence of the emergent gauge field and fractionalization will be another interesting topic.

Note Added: In the final stage of this work, we became aware of a related work arXiv:1909.07381 (Ref. [62]) discussing the dynamics of entanglement spectra.

W.Z. thank Xueda Wen for fruitful discussion and

Y. C. He for collaboration on a related project.

References

[1] Di Francesco P, Mathieu P, Sénéchal D 1997 *Conformal Field Theory, Graduate Texts in Contemporary Physics* (New York: Springer)
[2] Belavin A A, Polyakov A M and Zamolodchikov A B 1984 *J. Stat. Phys.* **34** 763
[3] Belavin A, Polyakov A and Zamolodchikov A 1984 *Nucl. Phys. B* **241** 333
[4] Friedan D, Qiu Z and Shenker S 1984 *Phys. Rev. Lett.* **52** 1575
[5] Cardy J L 1986 *Nucl. Phys. B* **270** 186
[6] Cardy J L 1986 *Nucl. Phys. B* **275** 200
[7] Srednicki M 1993 *Phys. Rev. Lett.* **71** 666
[8] Holzhey C, Larsen F and Wilczek F 1994 *Nucl. Phys. B* **424** 443
[9] Calabrese P and Cardy J 2004 *J. Stat. Mech.* **2004** P06002
[10] Korepin V E 2004 *Phys. Rev. Lett.* **92** 096402
[11] Calabrese P and Cardy J 2005 *J. Stat. Mech.* **2005** P04010
[12] Calabrese P and Cardy J 2006 *Phys. Rev. Lett.* **96** 136801
[13] Fradkin E and Moore J E 2006 *Phys. Rev. Lett.* **97** 050404
[14] Calabrese P and Cardy J 2007 *J. Stat. Mech.* **2007** P10004
[15] Calabrese P and Lefevre A 2008 *Phys. Rev. A* **78** 032329
[16] Hsu B, Mulligan M, Fradkin E and Kim E A 2009 *Phys. Rev. B* **79** 115421
[17] Calabrese P and Cardy J 2009 *J. Phys. A* **42** 504005
[18] Nienhuis B, Campostrini M and Calabrese P 2009 *J. Stat. Mech.* **2009** P02063
[19] Alba V, Tagliacozzo L and Calabrese P 2010 *Phys. Rev. B* **81** 060411
[20] Calabrese P, Campostrini M, Essler F and Nienhuis B 2010 *Phys. Rev. Lett.* **104** 095701
[21] Calabrese P, Cardy J and Tonni E 2012 *Phys. Rev. Lett.* **109** 130502
[22] Calabrese P, Cardy J and Tonni E 2013 *J. Stat. Mech.* **2013** P02008
[23] Cardy J 2014 *Phys. Rev. Lett.* **112** 220401
[24] Calabrese P, Cardy J and Tonni E 2015 *J. Phys. A* **48** 015006
[25] Coser A, Tonni E and Calabrese P 2014 *J. Stat. Mech.* **2014** P12017
[26] Cardy J 2016 *J. Stat. Mech.* **2016** 023103
[27] Calabrese P and Cardy J 2016 *J. Stat. Mech.* **2016** 064003
[28] Cardy J and Tonni E 2016 *J. Stat. Mech.* **2016** 123103
[29] Alba V, Calabrese P and Tonni E 2018 *J. Phys. A* **51** 024001
[30] Wen X, Ryu S and Ludwig A W W 2018 *J. Stat. Mech.* **2018** 113103
[31] Giudici G, Mendes-Santos T, Calabrese P and Dalmonte M 2018 *Phys. Rev. B* **98** 134403
[32] Giulio G D, Arias R and Tonni E 2019 arXiv:1905.01144[cond-mat.stat-mech]
[33] Vidal G, Latorre J I, Rico E and Kitaev A 2003 *Phys. Rev. Lett.* **90** 227902
[34] Pollmann F, Mukerjee S, Turner A M and Moore J E 2009 *Phys. Rev. Lett.* **102** 255701
[35] Metlitski M A, Fuertes C A and Sachdev S 2009 *Phys. Rev. B* **80** 115122
[36] Whitsitt S, Witczak-Krempa W and Sachdev S 2017 *Phys. Rev. B* **95** 045148
[37] Zhu W, Chen X, He Y C and Witczak-Krempa W 2018 *Sci. Adv.* **4** eaat5535
[38] Li H and Haldane F D M 2008 *Phys. Rev. Lett.* **101** 010504
[39] Laflorencie N 2016 *Phys. Rep.* **646** 1
[40] Fidkowski L 2010 *Phys. Rev. Lett.* **104** 130502
[41] Prodan E, Hughes T L and Bernevig B A 2010 *Phys. Rev. Lett.* **105** 115501
[42] Turner A M, Zhang Y and Vishwanath A 2010 *Phys. Rev. B* **82** 241102
[43] Qi X L, Katsura H and Ludwig A W W 2012 *Phys. Rev. Lett.* **108** 196402
[44] Thomale R, Arovas D P and Bernevig B A 2010 *Phys. Rev. Lett.* **105** 116805
[45] De Chiara G, Lepori L, Lewenstein M and Sanpera A 2012 *Phys. Rev. Lett.* **109** 237208
[46] Lepori L, De Chiara G and Sanpera A 2013 *Phys. Rev. B* **87** 235107
[47] Giampaolo S M, Montangero S, Dell'Anno F, De Siena S and Illuminati F 2013 *Phys. Rev. B* **88** 125142
[48] Lundgren R, Blair J, Laurell P, Regnault N, Fiete G A, Greiter M and Thomale R 2016 *Phys. Rev. B* **94** 081112
[49] Schuler M, Whitsitt S, Henry L P, Sachdev S and Läuchli A M 2016 *Phys. Rev. Lett.* **117** 210401
[50] Whitsitt S, Schuler M, Henry L P, Läuchli A M and Sachdev S 2017 *Phys. Rev. B* **96** 035142
[51] Stojevic V, Haegeman J, McCulloch I P, Tagliacozzo L and Verstraete F 2015 *Phys. Rev. B* **91** 035120
[52] Läuchli A M 2013 arXiv:1303.0741[cond-mat.stat-mech]
[53] Laflorencie N and Rachel S 2014 *J. Stat. Mech.* **2014** P11013
[54] Lieb E, Schultz T and Mattis D 1961 *Ann. Phys.* **16** 407
[55] Peschel I and Eisler V 2009 *J. Phys. A* **42** 504003
[56] Torlai G, Tagliacozzo L and Chiara G D 2014 *J. Stat. Mech.* **2014** P06001
[57] Vidal G 2004 *Phys. Rev. Lett.* **93** 040502
[58] Chepiga N and Mila F 2017 *Phys. Rev. B* **96** 054425
[59] Milsted A and Vidal G 2017 *Phys. Rev. B* **96** 245105
[60] Zou Y, Milsted A and Vidal G 2018 *Phys. Rev. Lett.* **121** 230402
[61] Zou Y and Vidal G 2019 arXiv:1907.10704[cond-mat.stat-mech]
[62] Surace J, Tagliacozzo L and Tonni E 2019 arXiv:1909.07381[cond-mat.stat-mech]